Absence of a gap in the infrared reflectance of Ni-doped $YBa_2Cu_3O_{7-\delta}$ films

Michael J. Sumner, Jin-Tae Kim, and Thomas R. Lemberger
Department of Physics, The Ohio State University, Columbus, Ohio 43210
(Received 2 November 1992)

We study the effects of Ni doping on the infrared reflectance of $YBa_2(Cu_{1-x}Ni_x)_3O_{7-\delta}$ films with up to 4% substitution of Cu by Ni. Normal-state spectra indicate that the primary effect of Ni on the conduction carriers is to increase their elastic scattering rate. At 4 at. % Ni, the elastic-scattering rate is calculated to be large enough to generate a large absorption onset at the gap edge in the superconducting state, if a gap exists. The superconducting-state spectra show no evidence for such a feature. Comparisons with phenomenological models for the optical conductivity show that the conductivity, and hence the superconducting density of states, is very gapless.

I. INTRODUCTION

A great deal of effort has been expended studying the infrared spectra of $YBa_2Cu_3O_{7-\delta}$, and other oxide superconductors, as reviewed extensively in Refs. 1 and 2. After this effort, interpretation of the optical properties of $YBa_2Cu_3O_{7-\delta}$ remains controversial for both the normal and superconducting states.

One interpretation is the "two-component" model in which the normal-state optical conductivity arises from a conventional conduction band plus a "midinfrared band" involving bound electrons of uncertain origin.[1] In this model, the scattering rate $1/\tau$ for conduction electrons is roughly $2kT/\hbar$ for $T > T_c$,[2] and it decreases more rapidly upon cooling into the superconducting state.[3–5] Hence, at low temperatures $T << T_c$, $\hbar/\tau$ is so much smaller than the superconducting energy gap $2\Delta(0)$ that the absorption onset at the gap frequency would be too small to observe, even for a BCS gap.[6] In this model, all of the absorption observed at 10 K or lower is from the midinfrared band.

Another interpretation is the "one-component" model.[2] The normal-state optical conductivity arises from a single band of unconventional conduction carriers which are strongly coupled to an optically inactive boson of uncertain origin. The strong coupling generates an inelastic-scattering rate that increases linearly with frequency, and thereby accounts for the anomalously strong absorption observed in the midinfrared. The conduction carriers are responsible for absorption in the superconducting state. Small features in the reflectance spectra at 150 and 450 cm^{-1} are interpretated as gaps for excitations moving on the CuO chains and CuO_2 planes, respectively.

We discuss our data in terms of the two-component model, comprising Drude conduction carriers plus a midinfrared band. Our conclusions do not depend on this choice. Previous workers[1,2] have applied this model to pure $YBa_2Cu_3O_{7-\delta}$ and found that the Drude conductivity corresponds well to the observed superconducting penetration depth $\lambda(0)=(m^*/ne^2\mu_0)^{1/2}\approx 160$ nm and normal-state resistivity $\rho(T)=m^*/ne^2\tau\approx 0.8\ \mu\Omega\,\mathrm{cm}\ (T/\mathrm{K})$, where m^* is the effective band mass and n is the density of conduction carriers. In other words, when the midinfrared band is subtracted from the experimental conductivity found by Kramers-Kronig analysis, the height and width of the remaining Drude peak correspond to the measured resistivity and to a scattering rate $\tau^{-1}(T)=\rho(T)/[\mu_0\lambda^2(0)]$.

We need to make an assumption about how the midinfrared band responds to Ni doping at the 4 at. % level. There is as yet no accepted model which would enable us to make physical estimates. Hence, we appeal to the spectra of Orenstein *et al.*[7] on oxygen-depleted $YBa_2Cu_3O_{7-\delta}$ twinned crystals. Interpreting their conductivities at $T << T_c$ as the midinfrared band, we see that oxygen depletion monotonically reduces its magnitude without affecting its frequency dependence. Reducing T_c to 50 K, by removing one-third of the chain oxygens to reach $O_{6.6}$, halves the midinfrared band conductivity for $\nu < 2000$ cm^{-1}. Two comments are in order. First, analysis of our data with a midinfrared band anywhere in this range leads to the same conclusions, primarily because the Drude conductivity is so much larger than the midinfrared band below about 400 cm^{-1}. Second, there is no evidence, either from doping levels, or T_c, or the Hall coefficient, that 4% Ni has an effect nearly as large as that of removing 33% of the chain oxygens. Therefore, we use for convenience the same T-independent Lorentz-oscillator parameterization of the midinfrared band which Kamaras *et al.*[6] used to fit their data on twinned $YBa_2Cu_3O_{7-\delta}$ films. This conductivity falls at the low end of the range found by Orenstein *et al.*[7]

II. Ni-DOPED $YBa_2Cu_3O_{7-\delta}$ FILMS

Information about $YBa_2(Cu_{1-x}Ni_x)_3O_{7-\delta}$ comes primarily from bulk ceramic samples.[8,9] The solubility limit is 10 at. %. As in Zn doping, the crystal remains orthorhombic, suggesting that the CuO chains remain intact and that a substantial fraction of the Ni goes into the CuO_2 planes. Smaller ionic radius dopants[10] such as Al, Co, and Fe make the lattice tetragonal above 4 at. %, and apparently strongly prefer chain sites. Direct determinations are difficult, and site preferences for Ni remain con-

troversial. T_c decreases monotonically, but $T_c(x)$ curves vary somewhat from group to group,[11] perhaps because different annealing procedures lead to different site preferences for Ni. In our films, the relatively short postannealing time of 1 h at a peak temperature of 900 °C, compared with weeks at comparable temperatures for ceramic samples, may favor random siting. In the end, $T_c(x)$ vs x for our films falls among curves reported for bulk ceramic samples.

Ni likely substitutes as Ni^{2+} for Cu^{2+}, so it should not affect the carrier density significantly. The Hall coefficients $R_H(T)$ for 3.3 at. % and 7 at. % Ni ceramics are identical to pure $YBa_2Cu_3O_{7-\delta}$ within the ±30% uncertainty imposed by ceramic samples.[12] In contrast, R_H for O-depleted $YBa_2Cu_3O_{7-\delta}$ with $T_c \approx 66$ K is about four times larger than for pure $YBa_2Cu_3O_{7-\delta}$.[12] 4 at. % Ni has a negligible effect on carrier density.

As discussed below, the dc resistivity of a patterned 3 at. % Ni $YBa_2(Cu_{1-x}Ni_x)_3O_{7-\delta}$ film (Fig. 2) indicates a residual resistivity of about 250 $\mu\Omega$ cm, and a corresponding elastic-scattering rate of about 250 $K \times k/\hbar$. (k is Boltzmann's constant.) The resistivity deduced from our reflectance spectra for 4 at. % Ni are about half of this, which we consider good agreement.

The films are made by codeposition of Y, BaF_2, Cu, and Ni onto (100) $SrTiO_3$ substrates in the presence of 3 microtorr of O_2, with a postanneal in moist oxygen at 900 °C.[13] The films are nominally 300-nm thick and about 1 cm in diameter. Thickness is determined from measurements on identically prepared patterned films. x is the nominal concentration of Ni from the measured Ni and Cu deposition rates. We have made good films up to 10 at. % Ni.

The structure of each film is characterized by x-ray diffraction, scanning electron microscopy (SEM), and Raman spectroscopy.[14] Powder x-ray diffraction indicates single-phase films highly oriented with the c axis perpendicular to the substrate. These results put an upper limit of about 10% on the volume of film consisting of misoriented grains and second phases. SEM micrographs show surface structure on a few percent of the sample surface, examples of which are in Ref. 13. This structure appears to be misoriented grains with dimensions ranging from 0.2 to 5 μm. These grains do not show up in Raman spectra, even though they should have much stronger Raman signals than the properly oriented grains. We conclude that misoriented grains do not extend deeply into the film. Raman also is very sensitive to some second phases with large Raman signals, such as $BaCuO_2$, but reveals none of these phases in the films. The overwhelming majority of the volume of our films consists of highly oriented grains of $YBa_2(Cu_{1-x}Ni_x)_3O_{7-\delta}$.

Figure 1 shows the low-frequency inductive response of films with up to 6% Ni. The ordinate is the change in the inductance of a tightly wound 10-turn 6-mm diameter pancake coil pressed gently against the sample film.[15] The maximum current density induced in the film is about 300 A/cm^2. These data have three important features. First, the onset of superconductivity is very sharp, as shown by the sharp "corner" at T_c. Poorer quality films show a rounded onset. Second, the transition widths are only a few percent of T_c, ensuring reasonable homogeneity. Third, $T_c(x)$ decreases linearly with increasing Ni concentration, demonstrating reproducibility of the fabrication technique. The rate of suppression of T_c with Ni doping is well within the range of values reported for bulk ceramic samples.[9–11]

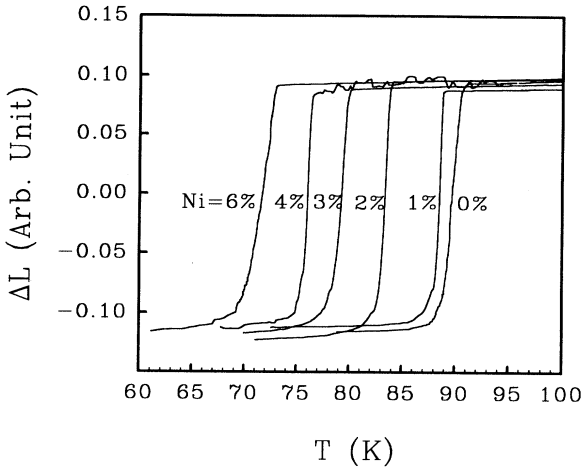

FIG. 1. Change in inductance of a pancake coil pressed against a film. The onset of superconductivity is sharp, and T_c decreases smoothly as Ni is added.

Figure 2 shows the resistivities of films made identically to those reported here, then patterned into strips.[13] Our pure $YBa_2Cu_3O_{7-\delta}$ films have resistivities $\rho(100\ K) \approx 100 \pm 20\ \mu\Omega$ cm; $\rho(T)$ extrapolates to zero at $T=0$, and the transitions are a couple of Kelvins wide. T_c ranges from 88 to 92 K. Figure 2 shows that 3% Ni in-

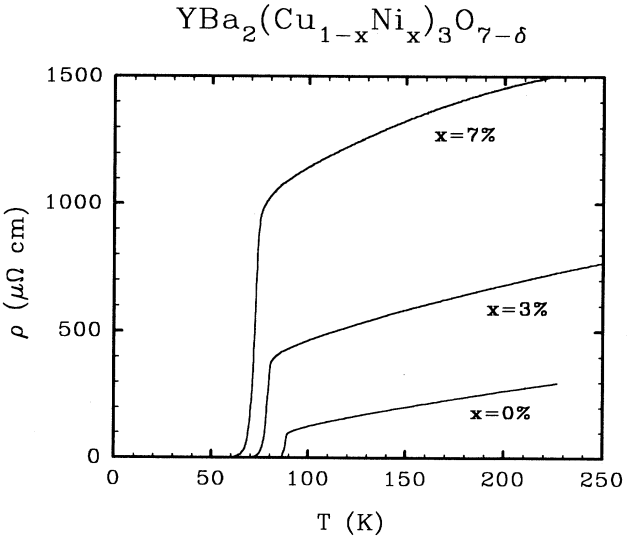

FIG. 2. Resistivities vs T of 0%, 3%, and 7% Ni-doped $YBa_2(Cu_{1-x}Ni_x)_3O_{7-\delta}$ films.

creases $\rho(T)$ and causes an apparent residual resistivity $\rho(0)\approx 250\ \mu\Omega$ cm. The data at 7% Ni continue this trend. For comparison, the resistivity of Zn-doped $YBa_2Cu_3O_{7-\delta}$ twinned crystals increases with Zn concentration at about half the rate we observe for Ni doping.[16]

We conclude that Ni-doped $YBa_2Cu_3O_{7-\delta}$ films are of sufficient quality to warrant extensive optical measurements. Although films are twinned and less well characterized than untwinned crystals might be, and transmission of some radiation through the film into the substrate precludes a Kramers-Kronig determination of the optical conductivity, still there are several important advantages of films for optical measurements. One is that some features in the reflectance are traceable to the $SrTiO_3$ substrate, which means that all of the film is probed by the radiation, not just the surface as for a crystal. Thus, the measured resistivity and inductive response of the film are those of the carriers reflecting the radiation. Another advantage is that, if there is an energy gap, then there is an interference between the reflectances of the film and the $SrTiO_3$ substrate which amplifies the calculated drop in reflectance at the gap frequency. Both of these advantages will be exploited below.

III. NORMAL-STATE REFLECTANCE SPECTRA

The reflectances of our films are measured with a Bomem Corp. Fourier transform spectrometer with a spot diameter of 7 mm and with an angle of incidence 11° from normal. The high value of the dielectric function $\epsilon(\omega)$ of $YBa_2Cu_3O_{7-\delta}$ in the infrared ensures that radiation in the film is polarized almost entirely in the plane of the film. The sample film and a Au mirror are mounted several centimeters apart on the cold finger of a helium-flow cryostat. The cold finger can be raised and lowered, thereby placing either the sample or the Au mirror in the optical path of the spectrometer. Typically, at each temperature several alternate measurements of film and Au mirror ensure an accurate determination of the relative reflectance of the sample. When Au mirrors are mounted at both locations on the cold finger, alternate measurements produce reflectances which agree within 1%. The difference is reproducible and is taken into account in our analysis.

Because some radiation penetrates through the films into the $SrTiO_3$ substrates, a Kramers-Kronig analysis does not produce accurate values for the optical conductivity of the films. Therefore, we compare our reflectance data with calculated model reflectances. The complete model for our samples comprises a conducting or superconducting film 300-nm thick on an infinitely thick $SrTiO_3$ substrate. This is a good approximation, since the actual substrate thickness of 1 mm is much larger than the longest wavelength of interest here. The spectrometer is run at a resolution of 4 cm^{-1} to average over the resonances due to standing waves in the substrate.

The normal-state optical response of the films comprises Drude carriers plus a broad midinfrared band, so that the complex conductivity is given by

$$\sigma(\omega)=\sigma_0/(1-i\omega\tau)+\sigma_{\rm MIR}(\omega)\ . \qquad (1)$$

The plasma frequency of the Drude carriers is taken to be $\nu_p/c=8200\ cm^{-1}$ ($\omega_p=1.55\times10^{15}$ rad/s; $\hbar\omega_p=1$ eV), independent of temperature and Ni concentration.[1] For reference, this value of ν_p yields $\lambda(0)=c/\omega_p=190$ nm, and for $\rho=100\ \mu\Omega$ cm, it corresponds to a scattering rate

$$1/\tau=\rho\epsilon_0\omega_p^2=2\times10^{13}\,s^{-1}=2\pi c\times106\,cm^{-1}$$
$$=160\,K\times k/\hbar\ . \qquad (2)$$

The midinfrared band is shown in Fig. 3. The peak value of the real part is about $(800\ \mu\Omega\ cm)^{-1}$. The lowest conduction carrier conductivity at dc is about $(500\ \mu\Omega\ cm)^{-1}$, for 4% Ni at 300 K. Hence, both the real and imaginary parts of the Drude conductivity dominate over the midinfrared band at low frequencies.

A four-parameter model of the measured conductivities and reflectances of $SrTiO_3$ at 300 and 85 K are shown in Figs. 4 and 5.[17] We use the 300-K data to model reflectances at 300 K and the 85-K data to model reflectances at 100 and 10 K. Note the strength and temperature dependence of the phonon at the lowest frequency; this phonon is apparent in our spectra and is very useful in determining the best-fit resistivity of our films. The phonons at 175 and 540 cm^{-1} are also present, but weaker.

Let us begin with pure $YBa_2Cu_3O_{7-\delta}$. Figure 6 shows reflectance spectra for $50<\nu<600\ cm^{-1}$ of a pure $YBa_2Cu_3O_{7-\delta}$ film at 10, 100, and 300 K. The solid curves are model calculations. Each data set is a superposition of spectra taken with different light sources, beam splitters, and detectors as appropriate for different frequency ranges. The noise level varies, being especially large near 200 and 550 cm^{-1}, but is about ±0.75% for most frequencies. In general, the film becomes more

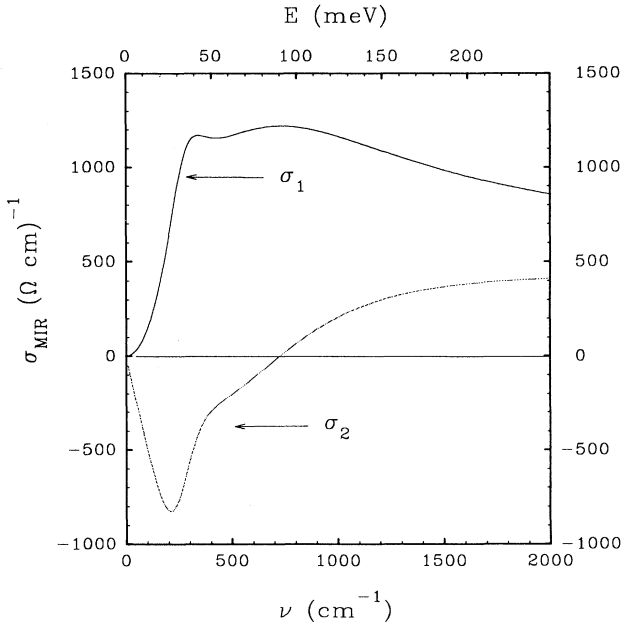

FIG. 3. Real and imaginary parts of the midinfrared band used to model our films.

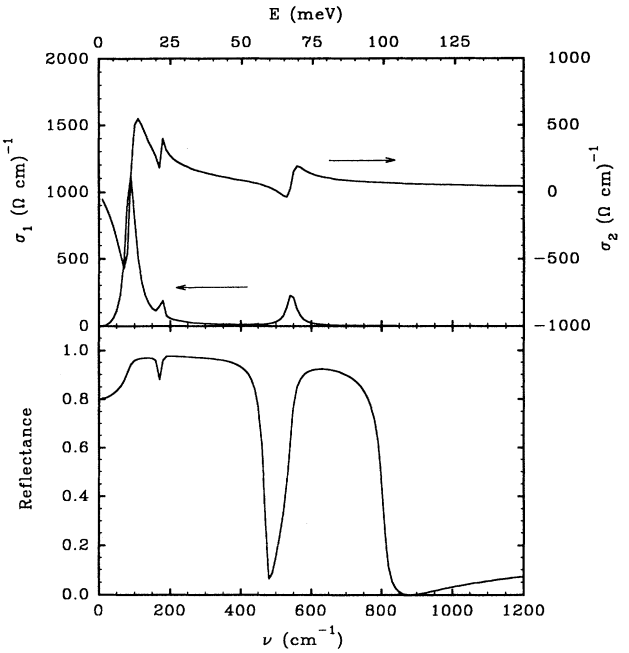

FIG. 4. Real part of the conductivity and reflectance of $SrTiO_3$ at 300 K.

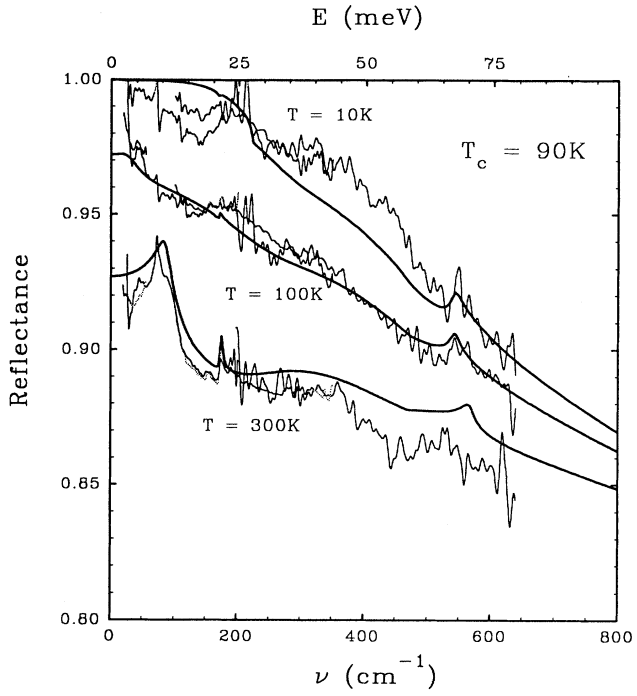

FIG. 6. Reflectance of a pure $YBa_2Cu_3O_{7-\delta}$ film at 10, 100, and 300 K. Solid curves are model calculations with $\rho(100\ \text{K}) = 125\ \mu\Omega\,\text{cm}$ and $\rho(300\ \text{K}) = 320\ \mu\Omega\,\text{cm}$.

reflective as it cools, as expected from a reduced resistivity. At 10 K, the film is nearly perfectly reflecting at the lowest frequencies. Apparently the surface structure observed under the SEM does not affect the film reflectance here.

Now consider more detail. The 300 K reflectance does not turn up toward unity at low frequency as expected for conductors. Instead, it has a maximum at $\nu \approx 100\ \text{cm}^{-1}$. The model calculation, which uses $\rho(300\ \text{K}) = 320\ \mu\Omega\,\text{cm}$, reveals that this feature arises from radiation passing through the film and interacting with the $SrTiO_3$ phonon at 80 cm^{-1}. At 100 K, the feature is softened because the film is less resistive [the model calculation uses $\rho\ (100\ \text{K}) = 125\ \mu\Omega\,\text{cm}$], so less light gets into the substrate. At 10 K, the model calculation uses a gap $2\Delta = 220\ \text{cm}^{-1} = 3.5kT_c$ and $\rho = 10\ \mu\Omega\,\text{cm}$. This is the clean limit, so the optical conductivity of the superconducting carriers is a δ function at $\nu = 0$. The reasonable agreement justifies our choice of midinfrared conductivity.

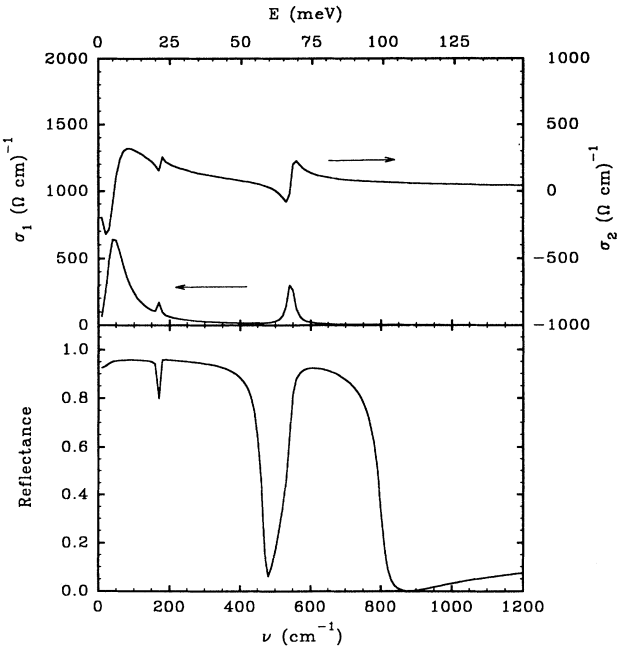

FIG. 5. Real part of the conductivity and reflectance of $SrTiO_3$ at 85 K.

Figure 7 shows reflectance spectra for a 1% Ni film at 10, 100, and 300 K. The 100 and 300 K spectra are different from those of pure $YBa_2Cu_3O_{7-\delta}$, but not by very much. The model calculations use the same resistivities, $\rho(300\ \text{K}) = 320\ \mu\Omega\,\text{cm}$ and $\rho(100\ \text{K}) = 125\ \mu\Omega\,\text{cm}$. The reflectance should be almost identical to pure $YBa_2Cu_3O_{7-\delta}$ at such a low doping level, so differences indicate the "noise" from sample-to-sample variations. We will see that the gap feature expected from these films is much larger than sample-to-sample variations.

Figure 8 shows reflectance spectra for a 2% Ni film over a wide frequency range. The data above 1000 cm^{-1} show that the doped films behave the same as undoped $YBa_2Cu_3O_{7-\delta}$ in this range, becoming steadily less reflective. Below 600 cm^{-1}, this film is not quite as reflective as pure $YBa_2Cu_3O_{7-\delta}$, and its reflectance does

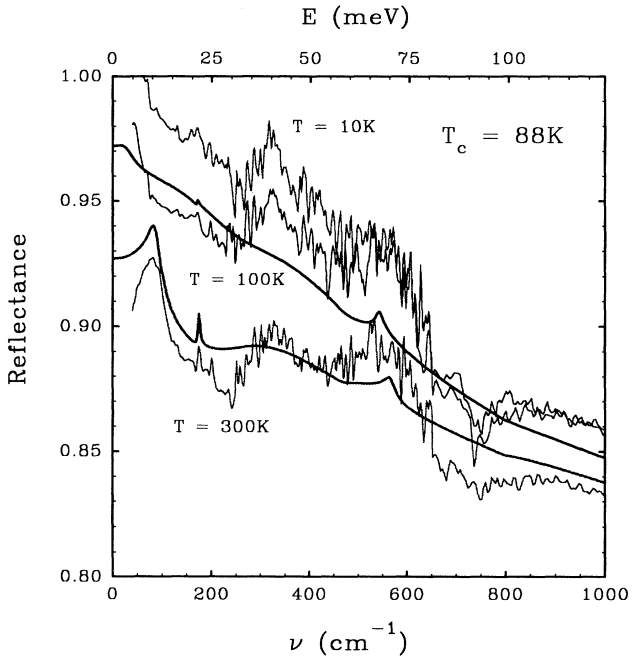

FIG. 7. Reflectance of a $YBa_2(Cu_{0.99}Ni_{0.01})_3O_{7-\delta}$ film at 10, 100, and 300 K. Solid curves are model calculations with ρ(100 K) = 125 $\mu\Omega$ cm and ρ(300 K) = 320 $\mu\Omega$ cm.

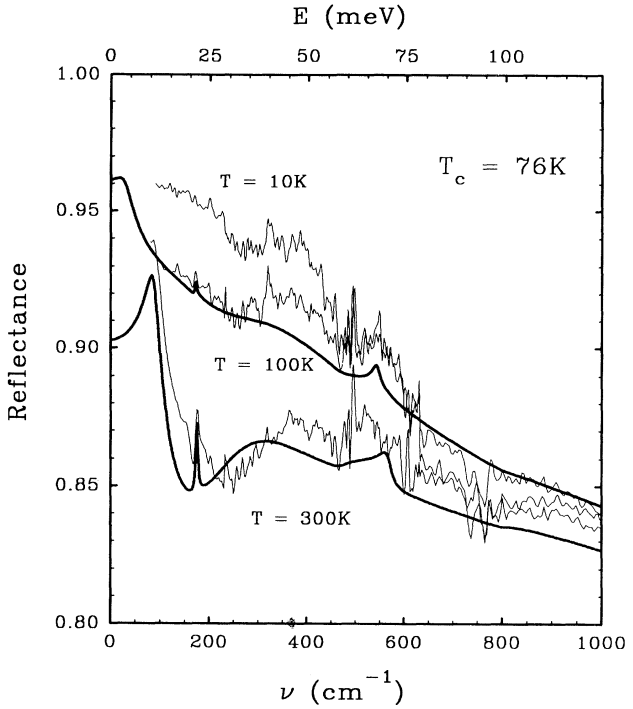

FIG. 9. Reflectance of a $YBa_2(Cu_{0.96}Ni_{0.04})_3O_{7-\delta}$ film at 10, 100, and 300 K. Solid curves are model calculations with ρ(100 K) = 220 $\mu\Omega$ cm and ρ(300 K) = 520 $\mu\Omega$ cm.

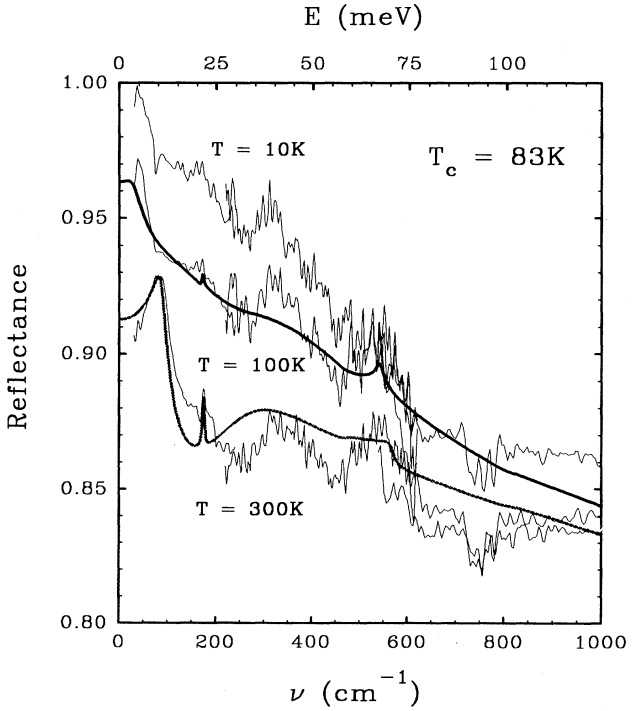

FIG. 8. Reflectance of a $YBa_2(Cu_{0.98}Ni_{0.02})_3O_{7-\delta}$ film at 10, 100, and 300 K. Solid curves are model calculations with ρ(100 K) = 200 $\mu\Omega$ cm and ρ(300 K) = 480 $\mu\Omega$ cm.

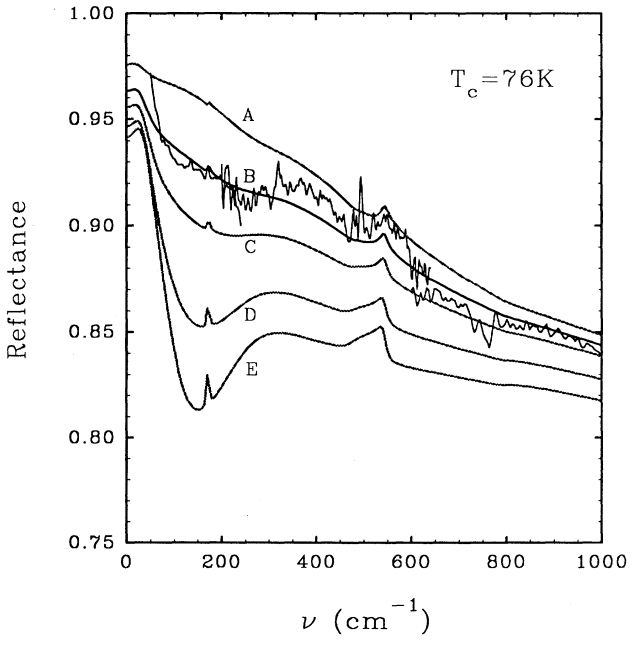

FIG. 10. Reflectance of a $YBa_2(Cu_{0.96}Ni_{0.04})_3O_{7-\delta}$ film at 100 K with model calculations for ρ = 100, 200, 300, 500, and 700 $\mu\Omega$ cm, curves A–E, respectively.

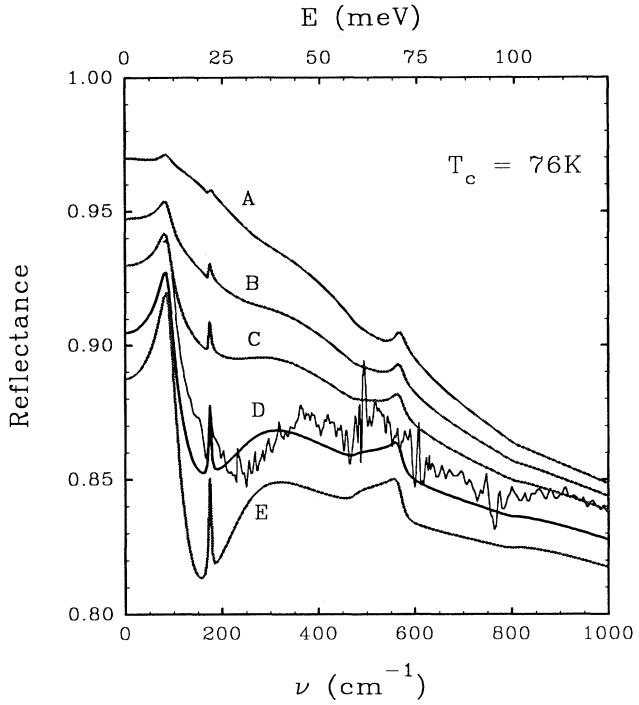

FIG. 11. Reflectance of a $YBa_2(Cu_{0.96}Ni_{0.04})_3O_{7-\delta}$ film at 300 K with model calculations for $\rho=100$, 200, 300, 500, and 700 $\mu\Omega$ cm, curves A–E, respectively.

not increase as much when it cools from 300 to 100 K. Model calculations, using $\rho(300\ \text{K})=480\ \mu\Omega$ cm and $\rho(100\ \text{K})=200\ \mu\Omega$ cm, show that these features indicate a higher resistivity, as expected.

Figure 9 shows the reflectance of a 4% Ni film. The decreased reflectances at 300 and 100 K relative to pure $YBa_2Cu_3O_{7-\delta}$ are described well by an increase in resistivity to $\rho(300\ \text{K})=520\ \mu\Omega$ cm and $\rho(100\ \text{K})=220\ \mu\Omega$ cm. Let us quantify the uncertainty in the optical determination of the resistivity. Figures 10 and 11 show the 100 and 300 K spectra for 4% Ni with curves calculated for several different resistivities. The most important feature in determining the best-fit resistivity is the steep drop below 100 cm^{-1} because the Drude conductivity is much larger than the midinfrared band in this range. The best fits are for $\rho=220\pm50\ \mu\Omega$ cm and $520\pm50\ \mu\Omega$ cm, respectively. These values are 100 and 200 $\mu\Omega$ cm larger than for pure $YBa_2Cu_3O_{7-\delta}$. We conclude that $100\pm50\ \mu\Omega$ cm is a reasonable estimate of the residual resistivity introduced by 4% Ni. This is somewhat less than the 250 $\mu\Omega$ cm inferred from the dc resistivity of a 3 at. % Ni film (Fig. 2), but in reasonably good agreement.

IV. SUPERCONDUCTING-STATE REFLECTANCE SPECTRA

The spectra at 10 K (Figs. 6–9) show that the films become gradually less reflective below 600 cm^{-1} as Ni is added. More significantly, no sharp features emerge. Since the spectra are similar, we will concentrate our analysis on the 4% Ni film because it has the largest scattering rate.

First of all, let us calculate what would occur if all of the conduction carriers condensed into a conventional superconducting state. We obtain the frequency dependence of the conductivity from the theory of Chang and Scalapino[18] (CS) for layered superconductors with weak electron-boson coupling. In the CS theory, currents are constrained to flow parallel to the planes so the anomalous skin effect does not occur for long mean free paths. The CS model applies at all temperatures and for electron-scattering rates ranging from clean $\hbar/\tau << 2kT_c$ to dirty $\hbar/\tau >> 2kT_c$ limits. Of course, area missing from the optical conductivity at finite frequencies is found in a δ function at zero frequency. We examine dc conductivities of $\sigma_0=1/50$, $1/100$, and $1/150\ \mu\Omega$ cm, corresponding to $1/\tau\approx53$, 106, and 160 cm^{-1}, respectively. The complete model includes the midinfrared band and an infinitely thick $SrTiO_3$ substrate.

Figure 12 shows the reflectance of the 4% Ni film at 10 K together with curves calculated for $2\Delta=185$ cm$^{-1}=3.5kT_c$ ($T_c=76$ K) and various resistivities. Figure 13 shows the same data with curves calculated for $2\Delta=400$ cm$^{-1}=7.6kT_c$. Note that the abrupt rise at about 70 cm^{-1} in the measured reflectance is associated with a substrate phonon which behaves differently in different substrates. Also, the "break" at 600 cm^{-1} in the measured reflectance is associated with uncertainty/noise

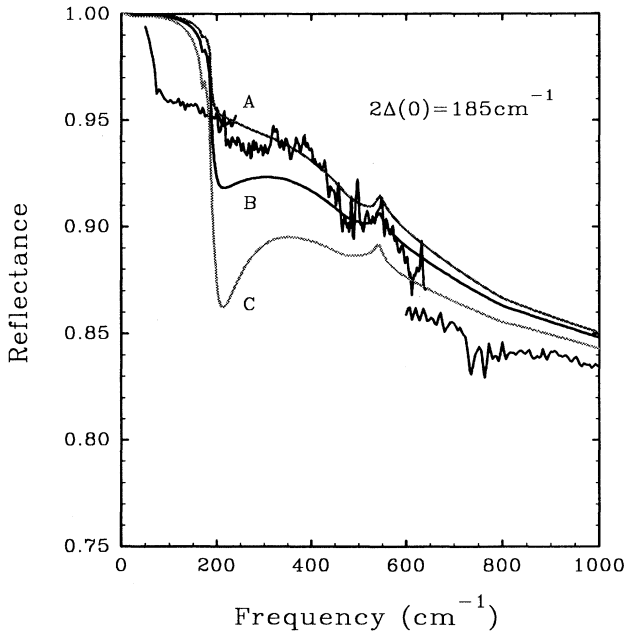

FIG. 12. Reflectance of a $YBa_2(Cu_{0.96}Ni_{0.04})_3O_{7-\delta}$ film at 10 K with model calculations for $2\Delta=185$ cm$^{-1}=3.5kT_c$ and $\rho=50$, 100, and 200 $\mu\Omega$ cm, curves A–C, respectively. Abrupt changes in reflectance at 70 and 600 cm^{-1} are artifacts associated with the substrate and a change in infrared detectors, respectively.

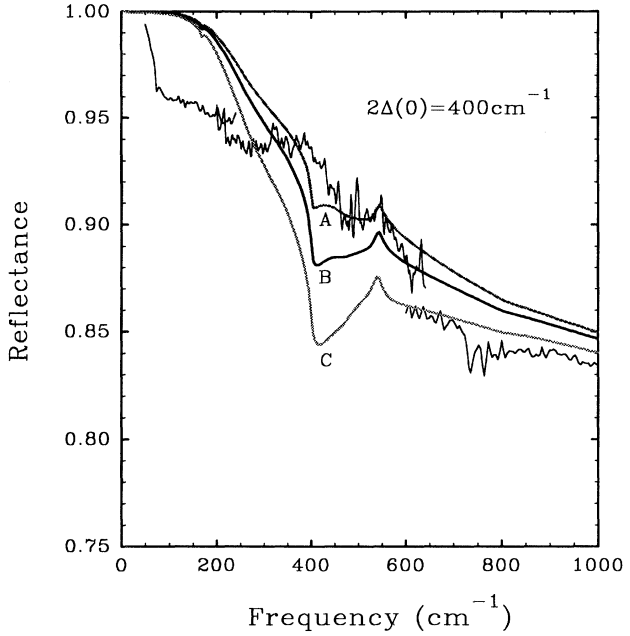

FIG. 13. Reflectance of a $YBa_2(Cu_{0.96}Ni_{0.04})_3O_{7-\delta}$ film at 10 K with model calculations for $2\Delta=400$ cm$^{-1}=7.6kT_c$ and $\rho=50$, 100, and 200 $\mu\Omega$ cm, curves A–C, respectively.

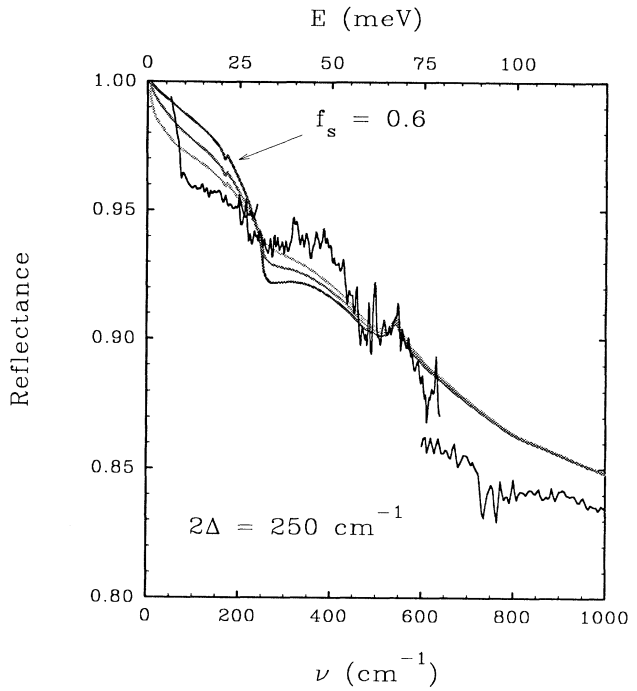

FIG. 14. Reflectance of a $YBa_2(Cu_{0.96}Ni_{0.04})_3O_{7-\delta}$ film at 10 K with two-fluid-model calculations for $f_s=0.2$, 0.4, and 0.6; $2\Delta=250$ cm^{-1}-$4.7kT_c$; and $\rho=100$ $\mu\Omega$ cm. The conductivities of the normal and superconducting carriers are shown in Fig. 15, labeled "normal drude" and "CS", respectively.

in the pyroelectric detector used above 600 cm^{-1}. Increasing 2Δ beyond 400 cm^{-1} moves the model into the clean limit in which absorption is entirely from the midinfrared band, so there is no gap feature. Note the steep drop between 200 cm^{-1} and $2\Delta(0)$ and the minimum at $2\Delta(0)$ in the calculated reflectances. The minimum results from interference between the responses of the substrate and film, as discussed in Ref. 19. We emphasize that such strong features could not be masked by whatever is responsible for the 1–2 % discrepancies between the model calculations and data in the normal state. They are absent. The conduction carriers do not condense into a BCS-like state with a sharply defined energy gap.

The question then becomes, how non-BCS must the superconducting state be? We proceed by comparing physically motivated phenomenological models for the conductivity of the superconducting electrons with the data. Of course, in each of these models area missing from the optical conductivity at finite frequencies resides in a δ function at zero frequency.

The simplest model is motivated by the idea that some of the carriers, e.g., those on the CuO chains, remain "normal" at low temperatures. Thus, the conductivity of the conduction carriers consists of a fraction f_s that go superconducting and have a gap and a fraction $1-f_s$ which remain normal. Figure 14 shows reflectances calculated for $f_s=0.2$, 0.4, and 0.6 superimposed on the 10 K spectrum of the 4% Ni film. While the best fit is for $f_s=0$, keeping in mind the differences between data and model in the normal state, we conclude that up to 40% of the carriers could go superconducting with a BCS-like density of states, if the other 60% remain normal. The calculated curve for 60% superconducting electrons is unacceptable primarily because it drops too steeply between 100 and 200 cm^{-1}, and secondarily because its absolute value at low frequency is higher than that observed. The steep drop arises from the abrupt increase in the real part of the conductivity at the gap frequency. Any theory with an abrupt feature superimposed on a smooth background conductivity will disagree with the data. The best-fit conductivity in this "two-fluid" model is very non-BCS in that at least 60% of the electrons remain normal. Note that a factor of 2.5 reduction in superfluid density implies that the penetration depth $\lambda(0)$ increases by a factor of $\sqrt{2.5}$ from pure $YBa_2Cu_3O_{7-\delta}$.

While we are considering coexisting normal and superconducting carriers, we should digress a moment to consider an inhomogeneous film with a putative normal layer on top of a superconducting layer. Model calculations of a three-layer system of normal film over superconducting film over substrate yield essentially the same results as the above calculation because infrared radiation penetrates through both layers. Thus, this type of inhomogeneity could explain our data only if the superconducting layer were less than 40% of the film thickness. Such a large inhomogeneity is not possible in our films.

Finally, let us examine phenomenological models in which the optical conductivity of the superconducting carriers is smooth, rather than having an abrupt feature at the gap edge. Perhaps then we can fit the data with a

conductivity below the "gap" which is significantly less than 60% of the normal-state conductivity.

Figures 15 and 16 show optical conductivities and corresponding reflectances ranging from completely superconducting ("CS") to completely normal ("Drude", for $\rho = 100\ \mu\Omega$ cm). The penetration depth $\lambda(0)$ is given for each case. $\lambda(0)$ increases as $\sigma_1(\nu)$ becomes more gapless. [In the clean limit, $\lambda(0)$ would be 190 nm.] The curve labeled "gapless" is similar to a conventional superconductor containing a high concentration of magnetic impurities.[20] We do not propose that Ni has a large magnetic effect. Such strong gaplessness at $T << T_c$ would require enough magnetic atoms to reduce T_c to less than 10% of the T_c of the host material, whereas 4% Ni reduces T_c by only 20%. We simply are comparing the phenomenological non-BCS conductivity to the data to see if it fits. It does not, (Fig. 16). Even the gentle rise in $\sigma_1(\nu)$ to a maximum at 250 cm^{-1} results in a reflectance which drops more steeply than the data in this range.

The curves labeled "very gapless" in Figs. 15 and 16 are roughly what one might obtain for a superconducting state with zeros of the order parameter along lines on the Fermi surface, or with a proximity effect between normal and "super" atomic planes.[21] This conductivity is similar to the two-fluid model with $f_s = 0.6$, but it is smoother and hence fits a little better (Fig. 16). Within uncertainties in the data and the model, the very gapless curve is an acceptable fit to the data.

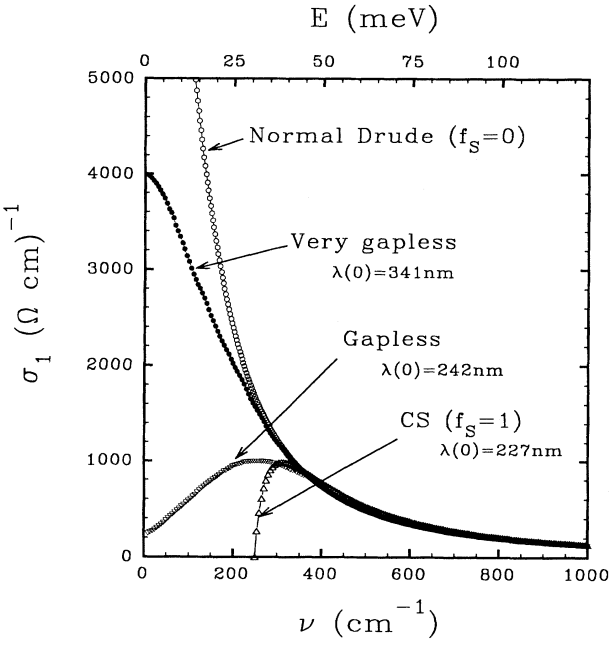

FIG. 15. Phenomenological conductivities for the superconducting carriers ranging from "normal drude" (with $\rho = 100$ $\mu\Omega$ cm and $1/\tau = 106$ cm^{-1}) to "very gapless" to "gapless" to completely superconducting "CS". For the latter three cases, area "missing" from the "Drude" curve is in a δ function at $\nu = 0$. The corresponding values of $\lambda(0)$ are given. In the clean limit, $\lambda(0) = 190$ nm for our choice of plasma frequency.

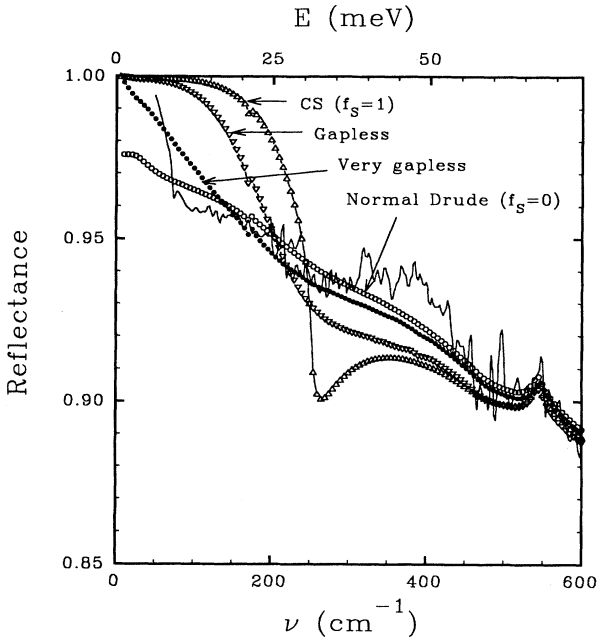

FIG. 16. Reflectance of a $YBa_2(Cu_{0.96}Ni_{0.04})_3O_{7-\delta}$ film at 10 K together with model calculations based on the conductivities in Fig. 15, with $2\Delta = 250\ cm^{-1} = 4.7kT_c$ and $\rho = 100\ \mu\Omega$ cm.

A recent theory[22] has an order parameter with *d*-wave symmetry, and therefore a gapless density of states. This theory has a very attractive feature missing in earlier simpler theories of *d*-wave superconductors, namely that it allows the elastic-scattering rate to exceed $kT_c/\hbar$ without driving T_c to zero. This could explain how our Ni-doped films can have scattering rates comparable to $kT_c/\hbar$ and T_c's above 75 K. It remains to be seen whether this theory can describe our infrared spectra. At this point we can conclude that, regardless of model, the data indicate a very non-BCS conductivity.

We conclude this section by considering the marginal Fermi-liquid theory. Nicol and Carbotte[23] have calculated the optical conductivity in the superconducting state for different scattering rates, with necessary assumptions about the effects of scattering on the parameters of the theory. They conclude that in pure $YBa_2Cu_3O_{7-\delta}$ the optical conductivity should have a sharp onset at $4\Delta(0)$. Elastic scattering should add another sharp onset at 2Δ, while reducing the onset at 4Δ. These qualitative features are confirmed in the detailed examination of Littlewood and Varma.[24] Neither of these sharp features is consistent with our data. Thus, even if we had analyzed our data in terms of a one-component model, we would have reached the same conclusions about the absence of a gap in the superconducting density of states.

V. SUMMARY AND CONCLUSIONS

We have measured the infrared reflectances of $YBa_2(Cu_{1-x}Ni_x)_3O_{7-\delta}$ films up to 4% Ni. Ni reduces T_c only slightly. A two-component model of the film

response explains the effect of Ni on the normal-state spectra entirely in terms of the dependence of the scattering rate of the conduction electrons on temperature and Ni concentration. The relatively flat and featureless reflectance spectra in the superconducting state can be understood in this framework only if the conduction electron response is very gapless and therefore very non-BCS.

Experimentally, we need data on more doped systems with other dopants with different spin states and site preferences. Measurements on doped crystals would be very useful, for comparison in the midinfrared range. Also, we need corroborating evidence through direct low-frequency measurements of the penetration depth, as well as measurements in the far infrared, where $\lambda(0)$ can be determined from the increase in reflectance toward unity that must occur even in very thin superconducting films.

ACKNOWLEDGMENTS

This work is based upon work supported in part by NSF Low-Temperature Physics Grant Nos. DMR 85-15370 and 88-22242 and from Ohio Edison Materials and Technology Centers. Substantial support for development of film fabrication and characterization techniques came additionally from AFOSR-91-0188 and DOE Grant No. DE-FG02-90ER45427 through the Midwest Superconductivity Consortium. We gratefully acknowledge discussions with David Tanner and Gordon Thomas.

[1]T. Timusk and D. B. Tanner, in *Physical Properties of High-Temperature Superconductors I,* edited by D. M. Ginsberg (World Scientific, New York, 1989), p. 339.

[2]D. B. Tanner and T. Timusk, in *Physical Properties of High-Temperature Superconductors III,* edited by D. M. Ginsberg (World Scientific, New York, 1992), p. 363.

[3]D. B. Romero *et al.*, Phys. Rev. Lett. **68**, 1590 (1992).

[4]M. C. Nuss, P. M. Mankiewich, M. L. O'Malley, E. H. Westerwick, and P. B. Littlewood, Phys. Rev. Lett. **66**, 3305 (1991).

[5]D. A. Bonn, P. Dosanjh, R. Liang, and W. N. Hardy, Phys. Rev. Lett. **68**, 2390 (1992).

[6]K. Kamaras *et al.*, Phys. Rev. Lett. **64**, 84 (1990); **64**, 1692 (1990).

[7]J. Orenstein *et al.*, Phys. Rev. B **42**, 6342 (1990).

[8]J. T. Markert, Y. Dalichaouch, and M. B. Maple, in *Physical Properties of High-Temperature Superconductors I,* edited by D. M. Ginsberg (World Scientific, New York, 1989), p. 265.

[9]L. H. Greene and B. H. Bagley, in *Physical Properties of High-Temperature Superconductors II,* edited by D. M. Ginsberg (World Scientific, New York, 1990), p. 509.

[10]D. M. Ginsberg, in *Physical Properties of High-Temperature Superconductors I,* edited by D. M. Ginsberg (World Scientific, New York, 1989), p. 1.

[11]Compare $T_c(x)$ curves from Fig. 28 of Ref. 8 and Fig. 24 of Ref. 9, for example.

[12]N. P. Ong, in *Physical Properties of High-Temperature Superconductors II,* edited by D. M. Ginsberg (World Scientific, New York, 1990), p. 459.

[13]J.-T. Kim, D. G. Xenikos, A. Thorns, and T. R. Lemberger, J. Appl. Phys. **72**, 803 (1992).

[14]K.-M. Ham, J.-T. Kim, R. Sooryakumar, and T. R. Lemberger, Phys. Rev. B (to be published).

[15]D. G. Xenikos and T. R. Lemberger, Rev. Sci. Instrum. **60**, 831 (1989).

[16]T. R. Chien, Z. Z. Wang, and N. P. Ong, Phys. Rev. Lett. **67**, 2088 (1991).

[17]A. S. Barker and M. Tinkham, Phys. Rev. **125**, 1527 (1962); **145**, 391 (1966).

[18]J.-J. Chang and D. J. Scalapino, Phys. Rev. B **40**, 391 (1989).

[19]M. J. Sumner, Ph.D. thesis, The Ohio State University, 1992 (unpublished).

[20]S. Skalski, O. Betbeder-Matibet, and P. R. Weiss, Phys. Rev. **136**, A1500 (1964).

[21]M. Frick and T. Schneider, Z. Phys. B **88**, 123 (1992).

[22]P. Monthoux, A. V. Balatsky, and D. Pines, Phys. Rev. B **46**, 14 803 (1992).

[23]E. J. Nicol and J. P. Carbotte, Phys. Rev. B **44**, 7741 (1991).

[24]P. B. Littlewood and C. M. Varma, Phys. Rev. B **46**, 405 (1992).